



Novel Evaluation of Intravoxel Incoherent Motion Using Fourier Analysis for Prostate Cancer Detection

Akio Ogura^{1*}, Fumie Maeda² and Katsumi Hayakawa³

Abstract

Introduction

To evaluate both a novel approach of data acquisition and the use of intravoxel incoherent motion (IVIM) as an analytical detection method in patients with prostate cancer.

Methods

This study retrospectively evaluated 34 patients who had prostate cancer diagnosed on biopsy. Diffusion-weighted images (DWIs) were obtained at specific values.

The IVIM diffusion model was used to ascertain the D^* , ADC, and perfusion fraction (f). The fitting curve was determined using the Fourier transform. An intercept value at 0.05 of the Fourier transform curve was defined as the vascularity-value (V-value). The V-values were compared with the D^* , f , and ADC.

Results

Prostate cancer detection rates on each index were $f = 0.59$, $D^* = 0.56$, $ADC = 0.78$, and $V\text{-value} = 0.74$. The rates of agreement obtained via a dynamic contrast enhanced (DCE)-MRI were $f = 0.53$, $D^* = 0.42$, and $V\text{-value} = 0.81$. The total prostate cancer detection rates using the ADC and V-value were 91%, in comparison with the total detection rates of both the ADC and DCE together.

Conclusion

A more detailed data acquisition is required for IVIM, and the Fourier transform was effective for evaluation of the IVIM curve shape. The V-value can be used to evaluate tumor vascularity.

Keywords

DWI; IVIM; MRI; Prostate cancer; V-value

Introduction

Prostate cancer is the most commonly diagnosed cancer and the second leading cause of cancer deaths in American men [1-3]. Commonly, prostate-specific antigen (PSA) testing is used for the screening of prostate cancer. Trans rectal ultrasonography (TRUS)-guided prostate biopsy is accepted as the gold standard for diagnosis, while the most important determiners of prostate cancer

prognosis are the Gleason score and tumor staging [4-6]. Magnetic resonance imaging (MRI) of the prostate provides excellent anatomic information, and this technique is considered sufficiently sensitive for prostate cancer detection. Generally, T2-weighted anatomical images of the gland are used to detect and stage prostate cancer. However, this method lacks specificity (<27%) in small tumors and cannot distinguish between prostate cancer and other lesions like prostatitis and benign prostatic hyperplasia [7,8]. In contrast, diffusion-weighted magnetic resonance imaging (DW-MRI) has been proven to improve prostate cancer detection.

Apparent diffusion coefficient (ADC) values are also important as regards to prostate cancer detection. The ADC values of cancerous prostate tissue are generally lower than those of normal prostate tissues, particularly in the peripheral zone (PZ). Normally, the ADC of water molecules within living tissues is derived analytically from diffusion images, with an assumption that the water molecular diffusion is a random process [9-17].

Dynamic contrast-enhancement MR imaging (DCE-MRI) can evaluate vascular characteristics. Increased micro vessel density will lead to an increase in blood flow, blood volume, and the surface area of vessel walls. An upturn in vascular endothelial growth factor production is likely to increase the permeability of these vessel walls. Blood flow, blood volume, and micro-vascular permeability-surface area product are all, in principle, quantifiable through analysis of contrast-enhanced MR imaging data by using distributed-parameter tracer kinetics models.

There are reports that intravoxel incoherent motion (IVIM) DWI may offer additional information regarding prostate cancer [18-24]. The IVIM model predicts a much faster diffusing exponential component in the signal equation due to perfusion effects, which affects the overall signal, predominantly at low b-values [25]. According to the IVIM DWI model, both pure extravascular molecular diffusion and microcirculation of blood within the capillaries (perfusion) can be separated using a bi-exponential decay function, providing additional parameters for tissue characterization.

The purpose of this study is to evaluate a novel method of data acquisition and an IVIM method using the Fourier analysis for detection of prostate cancer. First, the theory behind the method is explained, then this technique is applied and evaluated, through comparison with the DCE-MRI approach.

Materials and Methods

IVIM equation

$$S/S_0 = f \cdot \exp(-b \cdot (D^* + D)) + (1-f) \cdot \exp(-bD) \quad (1)$$

Here, S is the measured signal intensity, S_0 is the signal intensity without the influence of diffusion, D is the diffusion coefficient of water, and the sequence-dependent b-value characterizes the diffusion weighting. In addition, f is the perfusion fraction, D is the (molecular) diffusion coefficient, and D^* is the pseudodiffusion coefficient, which depends on the mean blood velocity and the mean capillary segment length. Since the mean blood velocity is considerably faster than the mean molecular diffusion velocity of water, the flow-related pseudodiffusion coefficient, D^* , is expected to be orders of magnitude

*Corresponding author: Akio Ogura, Graduate School, Gunma Prefectural College of Health Sciences 323-1, Kamioki-machi, Maebashi, Gunma, Japan, Tel: +81 27 235-1211; E-mail: a-ogura@mbox.kyoto-inet.or.jp

Received: June 02, 2016 Accepted: July 14, 2016 Published: July 20, 2016

greater than the tissue diffusion coefficient, D . As a consequence, the first term (the perfusion-related component) in Eq. (1) becomes very small for high b -values and, hence, perfusion effects are detectable at low b -values. The signal decay as a function of the diffusion b -value is thought to consist of three parts. The signal decay related b -values and f , D^* , and ADC are shown in (Figure 1).

The novel IVIM index

Generally, the evaluation of IVIM is based on the indices of f and D^* . The calculated values of D^* , f , and ADC on the mass and contralateral normal tissue of a patient with prostate cancer are shown in (Figure 2a). However, these indices may not always indicate the vascularity of the tissue [25]. Therefore, to overcome this limitation, we devised a novel IVIM index.

First, the small b -value data ($0 - 50 \text{ s/mm}^2$) were acquired in detail and used for IVIM analysis (Figure 2b). Then, curve fitting was applied to the diffusion signals in the form of an exponential curve using the least squares method. Next, this fitting curve was transformed using Fourier analysis. Finally, the intercept value at 0.05 of the vertical axis was taken as the new IVIM index, in the form of the vascularity-value (V -value) (Figure 3). Here, the Fourier analysis was used to analyze the shape of the fitting curve. In addition, we fixed Intercept value for 0.05 in consideration of a noise error of the signal acquisition.

Patients

In this study, the clinical and imaging data of 34 patients (age: 44-84 years; mean age: 67 years) with biopsy-proven prostate cancer were retrospectively evaluated. Ethical review board approval was obtained for this analysis, and informed consent was obtained from all patients. All of the 34 patients underwent a prostatectomy (after MR examination) and had biopsy-proved prostate cancer, with no relevant treatment history at the time of imaging (such as radiotherapy or chemotherapy). In addition, dynamic contrast material-enhanced (DCE) MR images were available for 24 patients.

MR images data acquisition

All images were acquired using the 1.5T clinical MRI system (Achieve; Philips Medical Systems, Best, the Netherlands) with a phased-array surface coil. All patients underwent a routine prostatic MR protocol, including diffusion-weighted images transverse to the prostate ($TR = 3,000 \text{ ms}$, $TE = 65 \text{ ms}$), with b -values of 0, 800, and $1,500 \text{ s/mm}^2$. DCE-MR images were obtained using a 3D fast-field echo sequence with a TR/TE of 3.8/1.9 ms and a flip angle of 15° . Pre-bolus images were taken, and 30, 60, 90, 120, 150, and 180 s after bolus, an IV injection of gadopentetate dimeglumine (Magnevist, Schering), followed by a 40-mL saline flush, and were sequentially detected by the DCE-MRI. The dosage of injected contrast material per patient was 0.1 mmol/kg of body weight, and the injection rate was 2 ml/s. IVIM DWI was performed before the DCE-MRI with a TR/TE of 6,000/120 ms, 4-mm slice thickness, a 128×128 matrix, and two excitations. Diffusion weighting was accomplished using a Stejskal-Tanner spin echo diffusion preparation with two monopolar diffusion gradient pulses, followed by a single-shot echo-planar imaging readout at b -values of 0, 5, 10, 15, 20, 25, 30, 35, 40, 50, 80, 100, 200, 400, and 800 s/mm^2 . For each b -value, diffusion weighted images were acquired with three orthogonal gradient directions, resulting in rotationally invariant trace images. A parallel imaging technique with sensitivity encoding was used to reduce the gradient-echo train lengths by a factor of 2. The acquisition time of the IVIM DWI was 12 min 43 s.

Image analysis

For each patient, the largest diameter region of interest (ROI) was placed in the tumors found and referenced as T2-weighted images and ADC maps, while another ROI was placed in contralateral healthy tissue on images with b -values of 15 (Figure 4).

The mean signal intensities over the ROIs were calculated for each b -value. According to the IVIM theory, the relative signal is given by Eq. (1) by means of a nonlinear least squares fit for solution of the D^* and f indices. The ADCs were calculated using the signals of the DW images with $b = 0$ and $1,500 \text{ s/mm}^2$. In addition, a mono-exponential fit curve using the images of $b = 0, 5, 10, 15, 20, 25, 30, 35, 40, 50 \text{ s/mm}^2$ was processed with the Fourier transform, and the intercept value at 0.05 of the Fourier transform curve was defined as the V -value.

Evaluation of dynamic contrast enhanced MRI

The signal intensity-time curves of dynamic contrast enhanced MRI were interpreted independently by three radiologists, who were blind to all patient information. The curves were evaluated to general perfusion parameters, including peak signal intensities, initial slope,

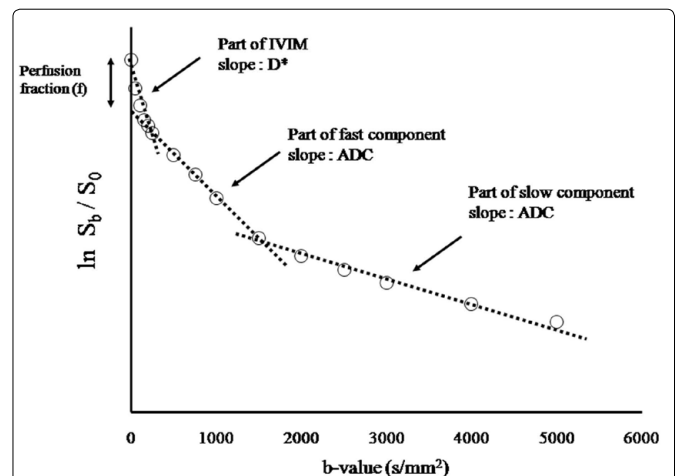


Figure 1: Decomposition of the tri-exponential relative signal decay as a function of the diffusion b -values. The dashed line indicates three-part decay: IVIM, fast component, and slow component.

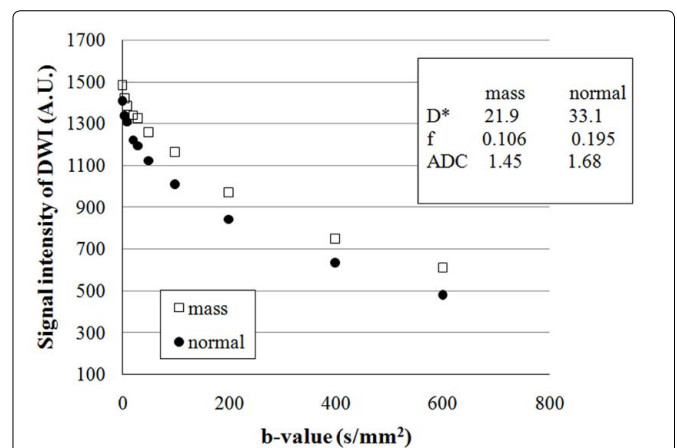
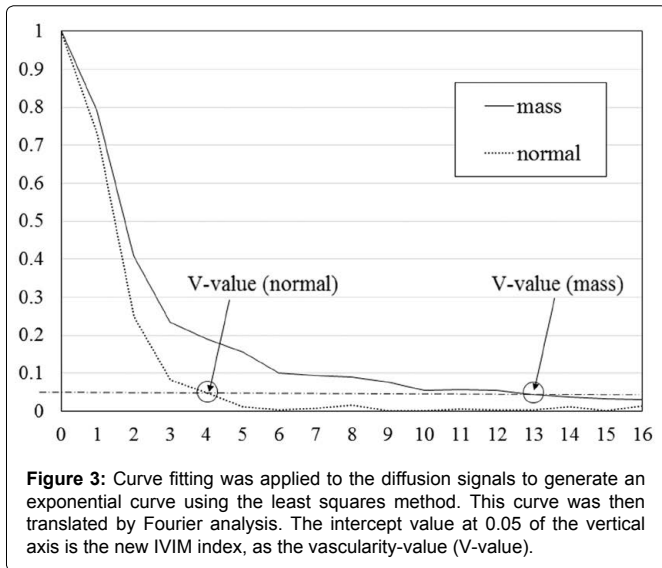
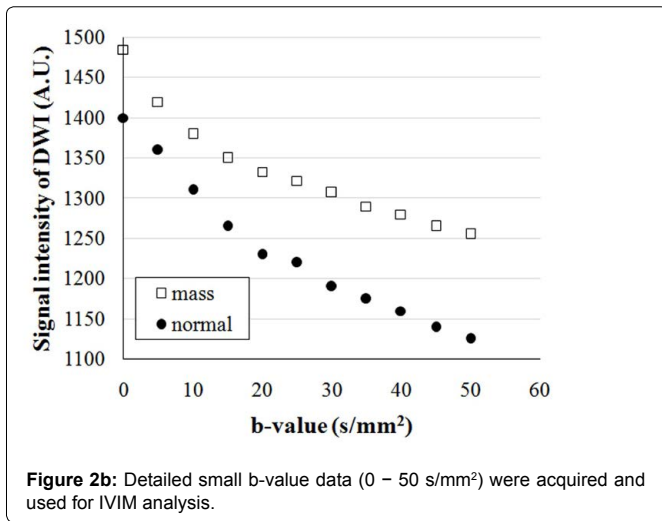


Figure 2a: Calculated values of D^* , f , and ADC on mass and contralateral normal tissue of patient with prostate cancer.



and maximum slope for the initial 50 s after the contrast injection, wash-in rate, and time-to-peak. The wash-in rate calculated it from the following equation.

$$\text{Wash-in rate} = (S_a - S_0) / S_a \cdot 1 / 30 \quad (2)$$

Here, S_a is the measured signal intensity of the initial 30 s after the contrast injection; S_0 is the signal intensity before the contrast injection.

The likelihood of the presence of cancer for the DCE-MRI images was indicated by a separately assigned score, using a five-point rating scale: 1 - not present; 2 - probably not present; 3 - possibly present; 4 - probably present; and 5 - definitely present. The averaged scores of the three radiologists were used as the DCE-MRI scores.

Evaluation of each index for IVIM

The index ratios of D' , f , ADC, and V-value are defined as the difference of each normal tissue and tumor index value divided by the mean, i.e.

$$\text{Index ratio} = (\text{Index value of normal} - \text{Index value of tumor}) / (\text{Index value of normal} + \text{Index value of tumor}). \quad (3)$$

The error of measurement range was defined as $\pm 1\%$, and any data not satisfying this requirement were excluded.

For the 34 patients with prostate cancer, the prostate cancer detection ratios of each index ratio (D' , f , ADC, and V-value) against the biopsy results were compared. The detection ratio is the numerical value that divided a positive number by a number judged to be malignant by biopsy.

In addition, the agreement ratios of the DCE-MRI score and each IVIM index ratio were evaluated.

Results

Differentiation between tumor and normal tissue using each index

The differences between the D' , f , and V-value results for the cancerous prostate tissue and contralateral normal tissue of the examined 34 patients are shown in (Figures 5-7).

At first, for evaluation of the measurement errors, the standard deviation of each index level of the normal tissue was calculated. This standard deviation defined an error of measurement range and appropriate data was excluded. The detection ratio of each IVIM index (ADC, D' , f , and V-value) against the biopsy results were ADC = 77%, D' = 53%, f = 56%, and V-value = 74% (Figure 8).

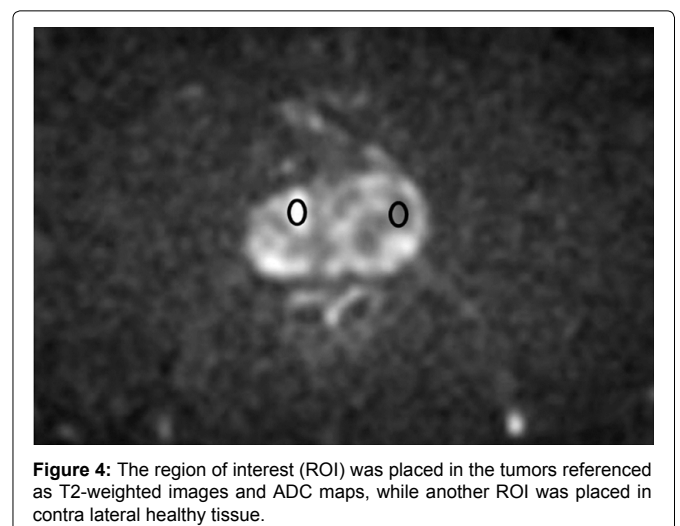
Agreement with dynamic contrast enhancement (DCE) evaluation and comparison of two complex indices

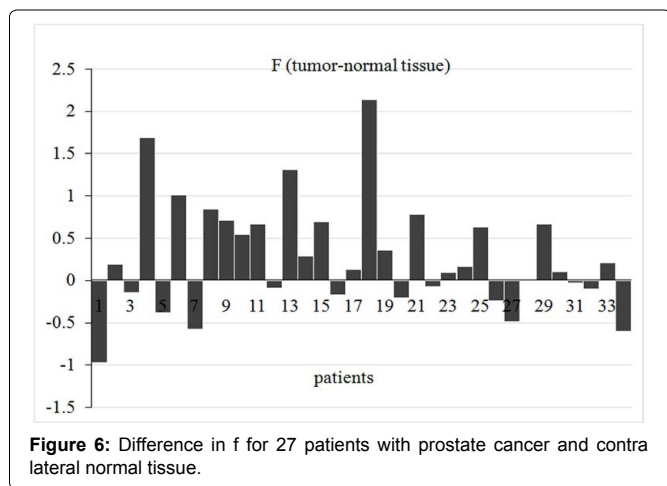
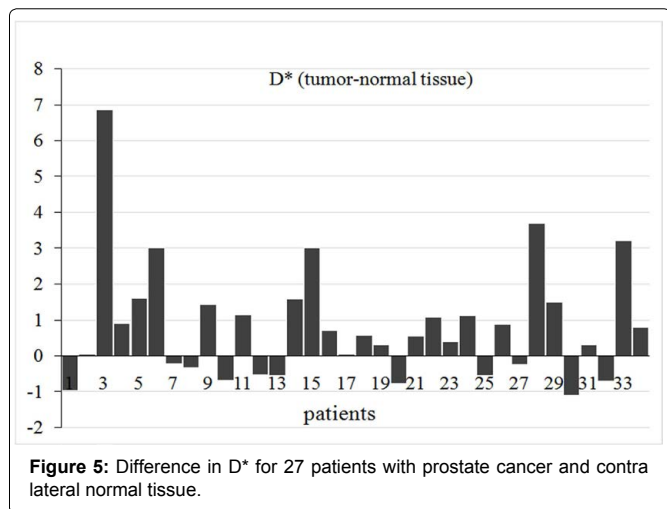
The agreement ratios of the DCE-MRI score and each IVIM index ratio were D' = 42%, f = 53%, and V-value = 81% (Figure 9).

When two indexes are combined, the detection rate increases more. In the combine of two indexes, both indexes case positive together was true positive. The detection rate obtained for the ADC and V-value indices was 85%, while the corresponding value for ADC and DCE-MRI was 93%. The detection rate of the ADC and V-value indices was 91% of the detection rate of the ADC and DCE-MRI indices together.

Discussion

As regards to the IVIM index, unlike the ADC, diagnostic information to reflect the vascularity of the tissue is obtained.





Therefore, if the IVIM method provides the same vascularity information as the DCE-MRI, it could be a useful means of reducing patient risk as, unlike DCE-MRI, so that contrast media are unnecessary for the application of this technique.

However, no literature was found that stated that f and D^* as IVIM indices sufficiently reflect the vascularity of a tumor. In addition, the acquisition and the analytical methods of the DWI low b -value data were found to be problematic. Therefore, we assumed that the low b -value data ($b = 0 - 50 \text{ s/mm}^2$) were detailed. Then, through the use of a non-linear least squares fit, these data were inserted into the IVIM equation and the fitting curve was processed using the Fourier transform. For evaluation of the IVIM curve shape, an intercept value at 0.05 of the Fourier transform curve was defined as the V -value.

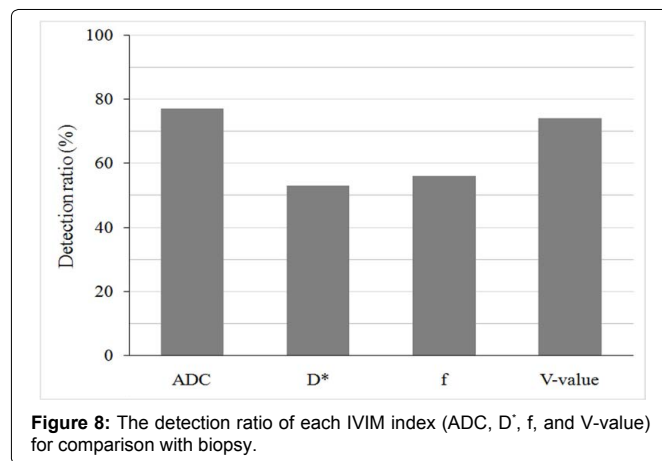
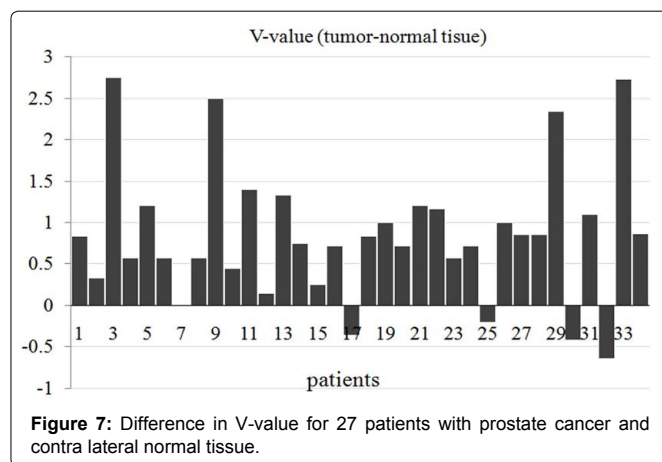
For the 34 patients with prostate cancer, the V -values of the novel index were compared with those of D^* and f in terms of tumor detection rates, and with the diagnostic information of DCE-MRI regarding tumor vascularity. As a result, the V -value detectability was found to be better than that of f and D^* , in comparison with the biopsy data. Therefore, the V -value was found to be effective as an IVIM index. The tumor detection method using both the ADC and V -value provided 91% accuracy, in comparison with the detection rate of both the ADC and DCE-MRI together. However, a case did exist in which it was impossible to detect the tumor using both the ADC and DCE-MRI, but was detectable using both the ADC and the V -value. These

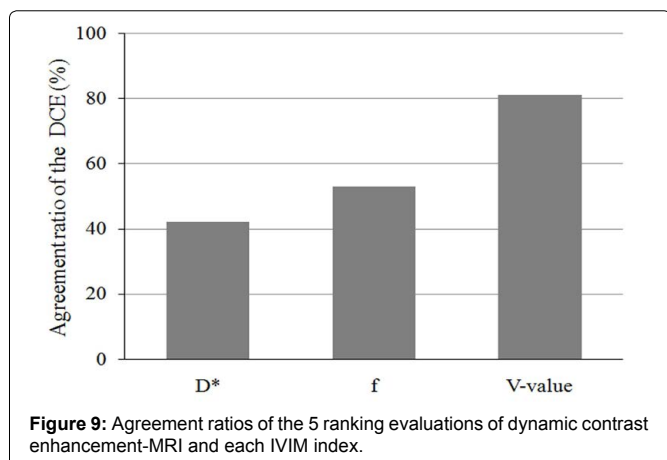
results indicate that the IVIM evaluation using the V -value is often superior to the DCE-MRI as regards to vascularity evaluation. For the DCE-MRI, the washout information contributes greatly to a diagnosis with perfusion information, but washout information cannot be obtained from IVIM using the V -value. Therefore, it is difficult to justify the use of IVIM alone instead of DCE-MRI. However, in the case of a patient for whom contrast media are unsuitable, much more diagnostic information can be obtained through the use of IVIM and the V -value. In addition, the diagnostic information can be further increased by adding IVIM to the DCE-MRI process.

Finally, as limitation of V -value, 0.05 was set in intercept value, but future examination is necessary for this numerical value.

Conclusions

More detailed data acquisition for low b -values was developed for IVIM, and these data were inserted into the IVIM equation using a non-linear least squares fit. The fitting curve was processed with the Fourier transform for evaluation of the IVIM curve shape. An intercept value at 0.05 of the Fourier-transform curve was defined as the V -value. It can be concluded that the V -value is effective as an IVIM index. Tumor detection using both the ADC and the V -value had 91% accuracy, in comparison with both the ADC and DCE-MRI. However, the V -value cannot be used to evaluate the washout, in contrast to the DCE-MRI, but it can be used to evaluate tumor vascularity. Therefore, the V -value approach can be used for patients for whom use of contrast media is not possible.





Declaration

All study participants provided informed consent, and the study design was approved by the appropriate ethics review boards. There are no conflicts of interest to declare.

References

1. Siegel R, Naishadham D, Jemal A (2012) Cancer statistics CA Cancer. *J Clin* 62: 10-29.
2. Chou R, Crosswell JM, Dana T, Bougatsos C, Blazine I, et al. (2011) Screening for prostate cancer: a review of the evidence for the U.S. Preventive Services Task Force. *Ann Intern Med* 155: 762-771.
3. Gofrit ON, Zorn KC, Taxy JB, Lin S, Zagaja GP, et al. (2007) Predicting the risk of patients with biopsy Gleason score 6 to harbor a higher grade cancer. *J Urol* 178: 1925-1928.
4. Eggener SE, Mueller A, Berglund RK, Ayyathurai R, Soloway C, et al. (2009) A multi-institutional evaluation of active surveillance for low risk prostate cancer. *J Urol* 181: 1635-1641.
5. Gleason DF (1966) Classification of prostatic carcinomas. *Cancer Chemother Rep* 50: 125-128.
6. Gleason DF, Mellinger GT (2002) Veteran's administration cooperative urological research group. Prediction of prognosis for prostatic adenocarcinoma by combined histological grading and clinical staging. *J Urol* 167: 953-958.
7. Nakashima J, Tanimoto A, Imai Y, Mukai M, Horiguchi Y, et al. (2004) Endorectal MRI for prediction of tumor site, tumor size, and local extension of prostate cancer. *Urology* 64: 101-105.
8. Claus FG, Hricak H, Hattery RR (2006) Pretreatment evaluation of prostate cancer using 3T MRI: comparison of T2-weighted and dynamic contrast-enhanced imaging. *J Comput Assist Tomogr* 30: 7-11.
9. Hambrock T, Somford DM, Huisman HJ, Oort IM, Witjes JA, et al. (2011) Relationship between apparent diffusion coefficient at 3.0T MR imaging and gleason grade in peripheral zone prostate cancer. *Radiology* 259: 453-461.
10. Desouza NM, Reinsberg SA, Scurr ED, Brewster JM, Payne GS (2007) Magnetic resonance imaging in prostate cancer: the value of apparent diffusion coefficients for identifying malignant nodules. *British journal of radiology* 80: 90-95.
11. Shimofusa R, Fujimoto H, Akamata H, Motoori K, Yamamoto S, et al. (2005) Diffusion-weighted imaging of prostate cancer. *J Comput Assist Tomogr* 29: 149-153.
12. Gibbs P, Pickles MD, Turnbull LW (2006) Diffusion imaging of the prostate at 3.0 tesla. *Investigative Radiology* 41: 185-188.
13. Oto A, Yang C, Kayhan A, Tretiakova M, Antic T, et al. (2011) Diffusion-weighted and dynamic contrast-enhanced MRI of prostate cancer: Correlation of quantitative MR parameters with gleason score and tumor angiogenesis. *Am J Roentgenol* 197: 1382-1390.
14. Peng Y, Jiang Y, Yang C, Brown JB, Antic T, et al. (2013) Quantitative analysis of multiparametric prostate MR images: Differentiation between prostate cancer and normal tissue and correlation with gleason score—a computer-aided diagnosis development study. *Radiology* 267: 787-796.
15. Mazaheri Y, Shukla-Dave A, Hricak H, Fire SW, Zhang J, et al. (2008) Prostate Cancer: Identification with combined diffusion-weighted MR imaging and 3D ¹H MR spectroscopic imaging – Correlation with pathologic findings. *Radiology* 246: 480-488.
16. Vargas HA, Akin O, Franiel T, Fire SW, Zhang J, et al. (2011) Diffusion-weighted endorectal MR imaging at 3 T for prostate cancer: Tumor detection and assessment of aggressiveness. *Radiology* 259: 775-784.
17. Turkbey b, Shah VP, Pang Y, Bernardo M, Xu S, et al. (2011) Is apparent diffusion coefficient associated with clinical risk scores for prostate cancers that are visible on 3-T MR images? *Radiology* 258: 488-495.
18. Pang Y, Turkbey B, Bernardo M, Kruecker J, Kadoury S, Merino MJ, et al. (2013) Intravoxel incoherent motion MR imaging for prostate cancer: An evaluation of perfusion fraction and diffusion coefficient derived from different b-value combinations. *Magn Reson Med* 69: 553-562.
19. Dopfert J, Lemke A, Weidner A, Schad LR (2011) Investigation of prostate cancer using diffusion-weighted intravoxel incoherent motion imaging. *Magn Reson Imaging* 29: 1053-1058.
20. Shinmoto H, Tamura C, Soga S, Shiomi E, Yoshihara N, et al. (2012) An intravoxel incoherent motion diffusion-weighted imaging study of prostate cancer. *Am J Roentgenol* 199: 496-500.
21. Mazaheri Y, Afaq A, Rowe DB, Lu Y, Dave AS (2012) Diffusion-weighted magnetic resonance imaging of the prostate: Improved robustness with stretched exponential modeling. *J Comput Assist Tomogr* 36: 695-703.
22. Le Bihan D, Breton E, Lallemand D, Aubin ML, Vignaud J, et al. (1988) Separation of diffusion and perfusion in intravoxel incoherent motion MR imaging. *Radiology* 168: 497-505.
23. Lima M, Le Bihan D (2016) Clinical intravoxel incoherent motion and diffusion MR imaging: Past, present, and future. *Radiology* 278: 13-32.
24. Zhang YD, Wang Q, Wu CJ, Wang XN, Zhang J, et al. (2015) The histogram analysis of diffusion-weighted intravoxel incoherent motion (IVIM) imaging for differentiating the Gleason grade of prostate cancer. *Eur Radiol* 25: 994-1004.
25. Andreou A, Koh DM, Collins DJ, Wallace T, Leach MO, et al. (2013) Measurement reproducibility of perfusion fraction and pseudodiffusion coefficient derived by intravoxel incoherent motion diffusion-weighted MR imaging in normal liver and metastases. *Eur Radiol* 23: 428-434.

Author Affiliations

¹Graduate School, Gunma Prefectural College of Health Sciences, Japan

²Department of Radiology, Kyoto City Hospital, Japan

³Department of Radiology, Iwate Prefectural Kamaishi Hospital, Japan

Submit your next manuscript and get advantages of SciTechnol submissions

- ❖ 50 Journals
- ❖ 21 Day rapid review process
- ❖ 1000 Editorial team
- ❖ 2 Million readers
- ❖ Publication immediately after acceptance
- ❖ Quality and quick editorial, review processing

Submit your next manuscript at • www.scitechnol.com/submission